Extensive screening and performance testing of nucleating agents for the sodium acetate trihydrate phase-change material

Jinjie Li, Michael A. Parkes and Christoph G. Salzmann[*]

Department of Chemistry, University College London, 20 Gordon Street, London WC1H 0AJ, United Kingdom.

ABSTRACT

Heat batteries often rely on phase-change materials that undergo phase transitions upon heat charging and release. Sodium acetate trihydrate (SAT) is considered one of the best phase-change materials in terms of storage capacity. Yet, it is well-known for supercooling which makes the search for effective nucleating agents a high priority. To perform extensive screening for nucleating agents and to test their performance, we designed a new instrument. The HeatMaster is capable of analyzing six samples on the gram-scale in parallel using the principle of power compensation which means that heat releases and uptakes can be obtained in a quantitative fashion. Out of the 36 tested nucleating agents, $CaCl_2 \cdot 2H_2O$ was identified as the best nucleating agent that outperforms several of the previously known nucleating agents in terms of temperature range of operation up to 80 °C. $CaCl_2 \cdot 2H_2O$ performs reliably as a nucleating agent for SAT down to 0.5 weight percent. $MgCl_2 \cdot 6H_2O$ was also identified as a nucleating agent. Yet, similar to the well-known $Na_2HPO_4 \cdot 12H_2O$, its performance is not reliable after heating to 80 °C. Out of the three nucleating agents, $CaCl_2 \cdot 2H_2O$ shows the best performance with respect to deterioration of the heat releases upon extensive thermal cycling with a maximum temperature of 65 °C.

1

Introduction

Heat batteries are important devices for storing thermal energy from heat pumps, solar and wind sources, off-peak electricity and industrial-waste heat.[1-7] Typically, the heat charging and release is achieved with the help of phase-change materials that undergo phase transitions. A wide variety of phase-change materials have been employed successfully including metal alloys, paraffins, fatty acids, sugar alcohols, ionic liquids and salt hydrates.[1, 4, 5, 8] Commercially viable phase-change materials should be cheap, display high-energy densities, release heat at a temperature suited for the application and their performance should remain as constant as possible during the life time of a heat battery. Compared to electrical batteries, heat batteries typically do not require expensive raw materials for their manufacture, such as lithium and cobalt, which is important for sustainability and environmental aspects.

Salt hydrates have received much attention as phase-change materials due to their high energy density as well as low price, flammability and toxicity.[5, 9-11] They are considered the best heat-storage materials with heat densities up to 514 MJ m^{-3}.[12] The heat uptakes or releases are observed at the melting points of the salt hydrates. A drawback associated with salt hydrates is their low thermal conductivity which can be addressed by creating composites with materials providing higher thermal conductivities.[9, 13] Liquid salt hydrates also often supercool which means that the heat releases are either delayed or not observed at all.[9] This problem can be addressed by adding appropriate nucleating agents. However, the search for effective nucleating agents is typically conducted on a trial and error basis, and the performance of nucleating agents may degrade over time.[14] Incongruent melting of the salt hydrates can also be problematic. This means that a salt hydrate melts to give a precipitate of its anhydrate or a hydrate with lower water content in addition to the liquid phase which consequently has a different chemical composition compared to the original hydrate.[9] Such effects can lead to phase separation, difficulties with rehydration upon heat release and ultimately performance losses of the heat batteries.[15] These problems can be minimized by mechanical agitation,[16] addition of thickeners[17-20] and microencapsulation.[21, 22] A further requirement for phase-change materials is a small volume change upon crystallization which would otherwise subject the heat batteries to undesirable mechanical stress.[14, 23] A general disadvantage of salt hydrates are their corrosive natures which means that leakages from heat batteries must be avoided.[24]

2

Sodium acetate trihydrate (SAT) is a popular salt hydrate that is used widely in commercial heat batteries and is well-known from its use in handwarmers.[25] It releases 226 - 264 J g^{-1} at a melting point of 58 °C which is a convenient temperature for domestic heating and hot tap water.[26-31] As can be seen in Figure 1, SAT melts incongruently to give a liquid solution and solid sodium acetate anhydrate (SAA). The peritectic point of SAT and SAA is found at about 57 w%.
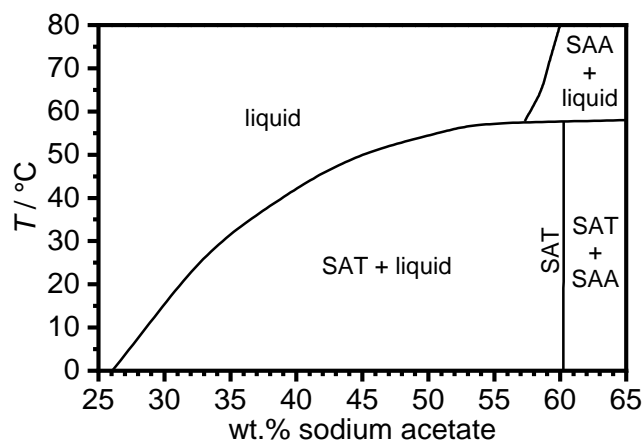
Figure 1. Binary phase diagram of sodium acetate and water including areas of stability of sodium acetate trihydrate (SAT) and sodium acetate anhydrate (SAA). Adapted from ref. 29, 32.

SAT is well-known for extensive supercooling.[14, 25] Yet, a variety of nucleating agents for SAT have been identified. These include $Na_4P_2O_7 \cdot 10H_2O$[27, 31, 33], sodium hydrogenphosphates such as Na_2HPO_4, $Na_2HPO_4 \cdot 7H_2O$ and $Na_2HPO_4 \cdot 12H_2O$.[17, 18, 27, 34], K_2SO_4,[35] Al_2O_3,[36] nano copper (10-30 nm),[37] silver nanoparticles,[38] AlN nanoparticles,[39] silicon carbide and bentonite,[40] activated charcoal,[41] expanded graphite[19] and chitin nanowhiskers.[42] Why certain materials nucleate SAT is unclear and it is also not well-understood why some materials become inactive upon heating to just a few tens of degrees above the melting point of SAT. Another concern is that an initially active nucleating agent may fail to work upon extensive thermal cycling over the lifetime of a heat battery.[43]

Differential scanning calorimetry (DSC) is often used for characterizing the supercooling and heat releases of phase-change materials. Yet, the amount of sample is typically only several tens of milligrams which is several orders of magnitude away from heat-battery applications. This means that supercooling effects and the problems associated with incongruent melting may

not be captured reliably.[30] Commercial DSCs can also typically only measure one sample at a time.

Gram-scale measurements of phase-change materials typically only measure the thermal history of samples.[42] This means that the sample temperature is recorded while a sample is cooled below the melting point of SAT. Upon crystallization, the sample temperature 'jumps' to the temperature of the melting point and further cooling is only observed once the sample has fully crystallized. Determining the heat release from such a setup in a quantitative fashion is difficult and it is not possible to enforce defined cooling rates.[42] On the plus side, due to the simplicity of the measurement, it is quite straight forward to conduct several experiments at the same time. The Galisol instrument contains about 10 g of a single phase-change material and can determine the latent heats of crystallization through careful calibration of the heat capacities of the various parts of the instrument.[14]

Here we design an instrument that is capable of characterizing six phase-change materials on the gram-scale in parallel using the principle of power compensation. In addition to crystallization temperature, the heat releases are determined in a quantitative fashion. Using the new instrument, we aim to identify new nucleating agents for SAT and to test their performance in detail upon extensive thermal cycling.

Experimental Section

Design of the HeatMaster instrument

A bespoke instrument for thermal cycling and performance-testing of phase-change materials was built. Our HeatMaster instrument characterizes six gram-scale samples in parallel and determines the heat releases or uptakes associated with phase transitions in a quantitative fashion. A photo of the entire setup and a schematic drawing of one of the six heating modules are shown in Figure 2(a) and (b), respectively. The heating modules (1) were machined from 40×40×55 mm aluminum blocks. A central cylindric cavity (2) accepts 10 mL glass vials (Samco soda glass specimen tubes with stopper 16×50 mm) containing the phase-change materials. The temperature of the aluminum block is measured close to the sample vial with a (3) Pt100 sensor in 4-wire configuration (RS Components, RS PRO PT100 RTD sensor, 2.8 mm diameter, 15 mm long, class A). The aluminum block is heated with (4) two resistive heating elements (Makers Hut, 24 V, 60 W, 6×20 mm ceramic cartridge heater) connected in parallel to a DC power supply (Tenma, model 72-2540, 30 V, 5 A)

4

with RS232 interface. Two M6 screws were inserted into the (5) holes of the aluminium blocks to firmly attached the heating modules to a (6) water-cooled aluminum cold sink separated by (7) 0.5 mm thick Teflon spacers.
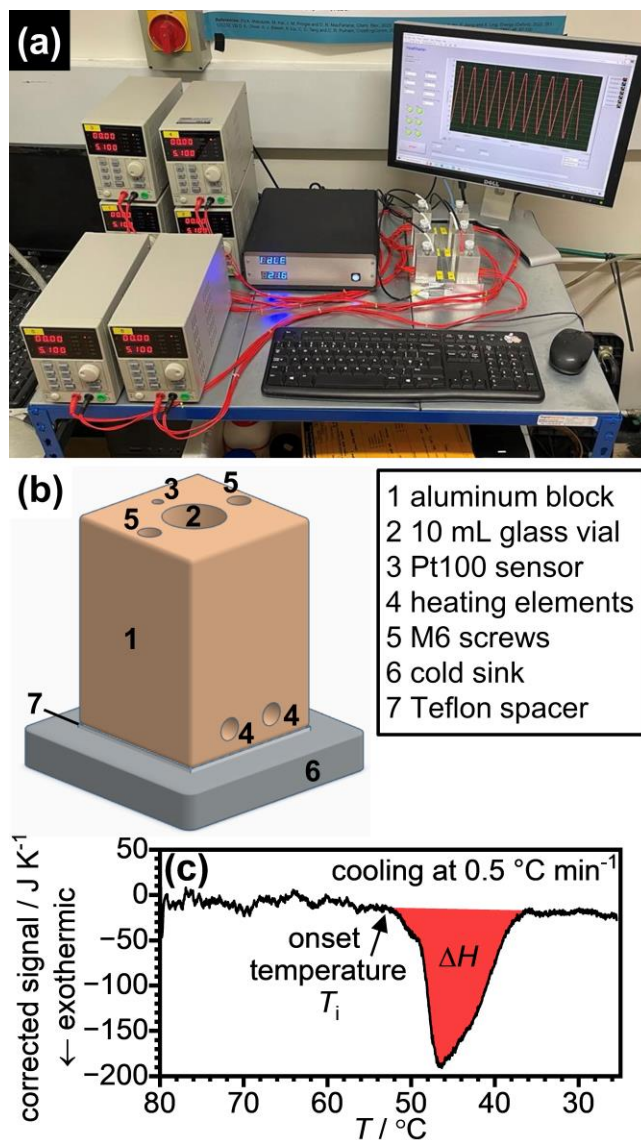
Figure 2. (a) Photographic image of the HeatMaster instrument. (b) Schematic rendering of one of the six heating modules with the locations of the various additional components indicated. (c) Background-corrected HeatMaster signal recorded upon cooling 5 g of sodium acetate trihydrate with nucleating agent at 0.5 °C min^{-1} from 80 to 25 °C. The exotherm due to the crystallization of sodium acetate trihydrate is shown as a red-shaded area and the onset temperature of crystallization, T_i, is indicated with an arrow.

5

The controller box of the HeatMaster contains one Adafruit Feather M0 Proto microcontroller for each of the six heating modules. The code for the various microcontrollers was written in C++ in the Arduino IDE. Specifically, the six microcontrollers were programmed to read the temperatures of the heating modules using Adafruit MAX31865 Pt100 amplifiers, to set the voltages of the power supplies via TTL-RS232 converters and to read the electric currents from the power supplies. Each microcontroller can accept a setpoint temperature which is then realized using a PID control algorithm with the Pt100 temperature as input and the voltage of the power supply as output (0 – 20 V).

An additional Adafruit Feather M0 acts as the master microcontroller and controls the six microcontrollers responsible for the individual heating modules. Within the master microcontroller, a temperature program is defined in terms of four stages including (1) dwelling at a base temperature for a specified period of time, (2) heating at a defined heating rate, (3) dwelling at the maximum temperature for a specified period of time and (4) cooling back to the base temperature at a defined cooling rate. These four stages constitute a cycle and can be repeated until the total number of specified cycles is reached. The setpoint temperatures from a defined temperature profile are sent to the six microcontrollers every second, and the voltages and currents required to follow the temperature profile are returned to the master microcontroller. Figure S1(a) shows the temperature profile of a typical experiment with 10 cycles, base temperature of 25 °C, maximum temperature of 80 °C, 0.5 °C min^{-1} as heating / cooling rates and using empty glass vials. The differences between the setpoint temperatures and the actual temperatures of the six modules are shown in Figure S1(b). It can be seen that the thermal lag upon heating and cooling is small and never exceeds 0.3 °C.

The electric power required to realize the temperature profile is calculated from the product of voltage and current. Figure S2 shows the power profiles required to run the six heating modules according to the temperature profile shown in Figure S1. Power variations between the six modules are attributed to small variations in the thicknesses of the Teflon spacers and different proximities to the inlet of the cooling water at the cold sink.

For the heating and cooling stages, the electric power was divided by the heating / cooling rate resulting in a signal with a unit of J K^{-1} which can then be plotted against temperature. Figure S3 shows such data recorded upon cooling an empty vial as well as a vial containing 5 g of SAT with a nucleating agent from 80 to 25 °C at 0.5 °C min^{-1}. As the sample releases heat upon

6

crystallization, the PID algorithm regulates back the voltage of the heating element so that the temperature profile is followed as closely as possible. This results in a negative deviation of the signal compared to the empty vial as highlighted by the arrow in Figure S3. The resulting exothermic feature is more clearly seen once the signal of the empty vial is subtracted as a background as shown in Figure 2(c). This resulting exothermic feature can then be integrated to obtain the crystallization enthalpy, ΔH, and the onset temperature of crystallization, T_i, can be determined as indicated by the arrow. The successful power compensation achieved by the PID algorithm during crystallization can be seen from the small temperature differences upon cooling an empty glass vial and a vial containing 5 g of SAT with nucleating agent in Figure S4.

Figure S5(a) shows the background-corrected cooling curves for vials containing different amounts of SAT ranging from 5 to 1 g. The obtained crystallization enthalpies are plotted against the mass of SAT in Figure S5(b). It can be seen that the HeatMaster shows a good linear response and the crystallization enthalpy per gram of SAT determined from the slope in Figure S5(b) is -202.9 ± 8.4 J g^{-1} which agrees with the values reported in the literature.[26-31]

As a safety feature, the master microcontroller also monitors the temperature of the cold sink and is programmed to immediately stop any heating of the six modules should the temperature exceed 30 °C.

Finally, a LabView program on a PC sends all the required experimental parameters to the master microcontroller to initiate a measurement, and it receives and records the actual temperatures of the modules as well as voltages and currents from each heating element over the course of the entire experiment. Our longest experiments so far lasted about 9 days with 50 temperature cycles.

Sample preparation for HeatMaster experiments

For a typical experiment, 5 g of SAT (Thermo Scientific, 99+%, extra pure) and 0.25 g of a potential nucleating agent were placed in a sample vial and thoroughly shaken. The vial was then sealed with PTFE tape around the plastic stopper and inserted into the HeatMaster. The standard heating profile involved thermal cycling between 25 and 80 °C at a rate of 0.5 °C min^{-1}, and dwelling times of 15 and 30 minutes at 25 and 80 °C, respectively. The maximum temperature was reduced to 65 °C for some experiments.

Powder X-ray diffraction

https://doi.org/10.26434/chemrxiv-2024-h5zqj ORCID: https://orcid.org/0000-0002-0714-7342 Content not peer-reviewed by ChemRxiv. License: CC BY-NC-ND 4.0

X-ray diffraction patterns were collected using a Stoe Stadi P X-ray diffractometer (Cu Kα1 radiation at 40 kV, 30 mA and monochromated by a Ge 111 crystal) equipped with a Mythen 1 K linear detector. The samples were carefully ground with a pestle and mortar, placed between greased acetate foils and clamped onto the sample holder which was rotated during the measurements. The diffraction patterns were collected over $2\theta = 2$ - $60°$ with $0.5°$ steps and 5 second accumulation times per step.

Results and Discussion

A total of 36 potential nucleating agents were tested with respect to their abilities to nucleate SAT upon cooling at 0.5 °C min^{-1} from 80 °C. These included several water-insoluble materials such as graphite, kaolinite, $BaSO_4$, SiC, $CaCO_3$ (calcite) and ZnS. Yet, the majority of tested nucleating agents were various salts and salt hydrates which may displays some solubility in the molten SAT. For all experiments, 5 g of SAT were used as well as 0.25 g of nucleating agent. The HeatMaster scans upon cooling are shown in Figure 3. Successful crystallization of SAT was only observed for two experiments using $CaCl_2 \cdot 2H_2O$ and $MgCl_2 \cdot 6H_2O$ as the nucleating agents. The crystallization exotherms are highlighted with red-shaded areas in Figure 3. To the best of our knowledge, these alkaline earth chloride hydrates have not yet been identified as nucleating agents for SAT. In all other cases, supercooling of liquid SAT solution was observed.

8
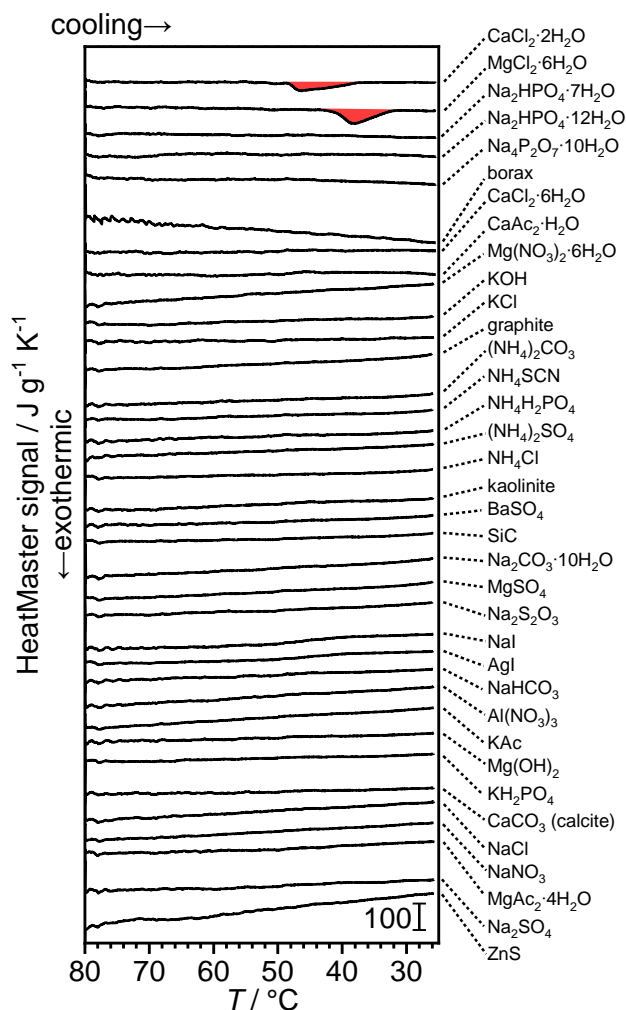
Figure 3. HeatMaster scans recorded upon cooling 5 g of sodium acetate trihydrate combined with 0.25 g of potential nucleating agent from 80 to 25 °C at 0.5 °C min^{-1}. The list of tested nucleating agents is given in the legend on the right-hand side of the figure. Crystallization exotherms were observed using $CaCl_2 \cdot 2H_2O$ and $MgCl_2 \cdot 6H_2O$ as nucleating agents as indicated by the red-shaded exothermic peaks.

The reliability of $CaCl_2 \cdot 2H_2O$ as a nucleating agent for SAT was tested in a next step. Figure 4 shows 10 heating / cooling cycles between 25 to 80 °C. The endothermic melting peaks are shown with a blue-shaded background in Figure 4(a). The first melting is shifted slightly towards higher temperatures which can be attributed to a poorer thermal conductivity of the initially loose powder. Figure 4(b) shows that nucleation of SAT takes place reliably for all ten cycles as indicated by the red-shaded exotherms and the reproducibility was confirmed with two additional samples also subjected to 10 heating / cooling cycles.
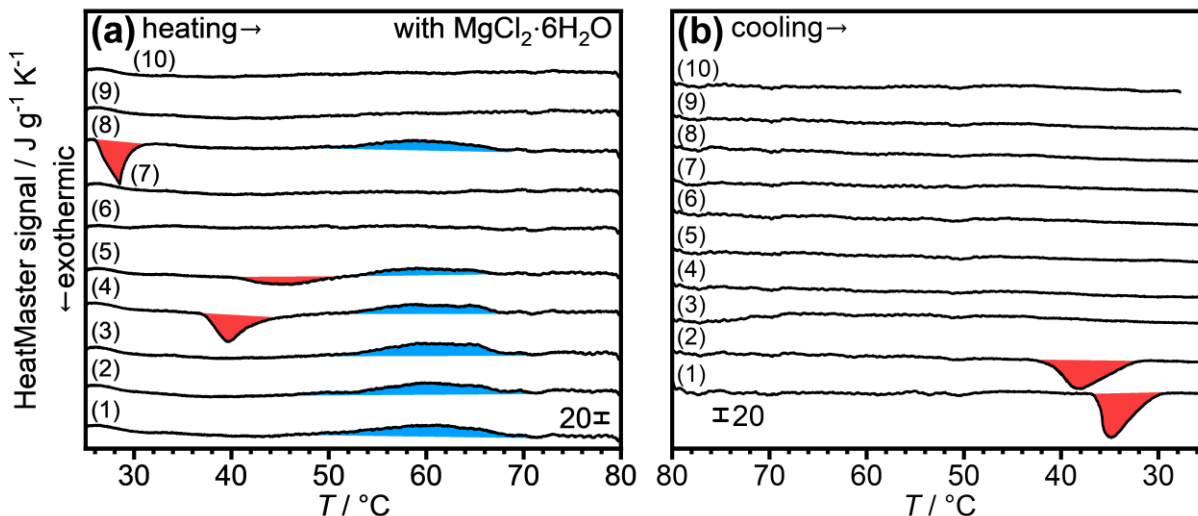
9
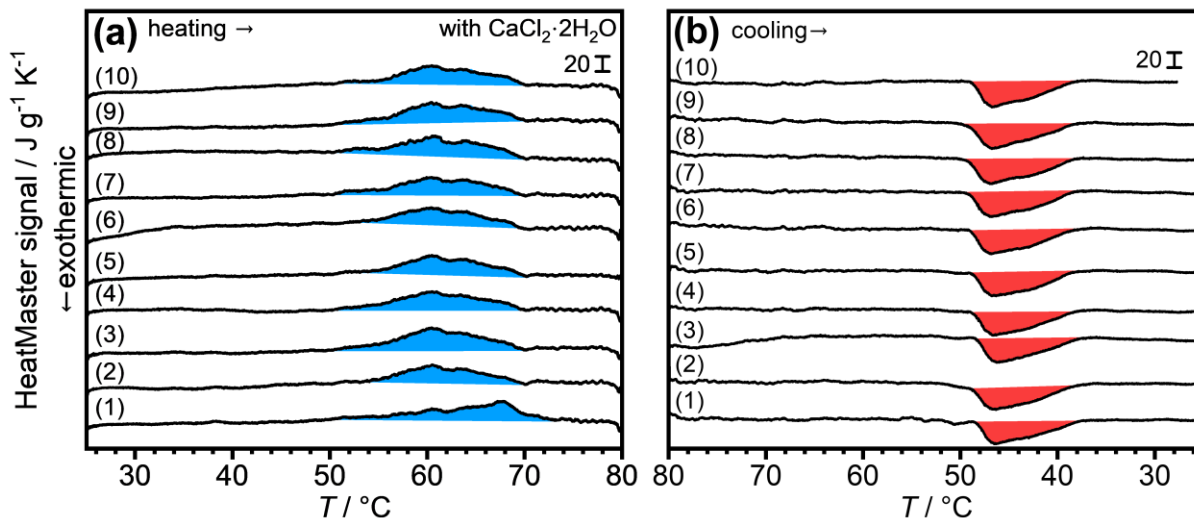
Figure 4. HeatMaster scans of 5 g sodium acetate trihydrate with 0.25 g $CaCl_2·2H_2O$ and 10 cycles. (a) Heating at 0.5 °C min^{-1} from 25 to 80 °C. (b) Cooling at 0.5 °C min^{-1} from 80 to 25 °C. Endotherms and exotherms are indicated by blue and red-shaded areas, respectively. The cycle numbers are given for each of the scans.

Upon reducing the amount of $CaCl_2·2H_2O$ from 0.250 g to 0.025 g while keeping the amount of SAT constant at 5 g, the crystallization exotherms continued to appear reliably as shown in Figure 5. These tests were again conducted with three individual samples each subjected to 10 heating / cooling cycles. Upon lowering the amount of $CaCl_2·2H_2O$ to 0.005 g, a slight shift of the exotherm towards lower temperatures was observed indicating that $CaCl_2·2H_2O$ becomes somewhat less effective as a nucleating agent. Finally, at 0.001 g $CaCl_2·2H_2O$, no exotherms were observed during 10 heating / cooling cycles and for three individual samples. It seems likely that this small amount of $CaCl_2$ becomes soluble in liquid SAT and is hence no longer able to provide a solid interface for the nucleation of SAT upon cooling. Accordingly, the minimal amount of $CaCl_2·2H_2O$ needed for reliable nucleation of SAT is around 0.1 w%. Yet 0.5 w% is probably the best choice if supercooling needs to be minimized.

10
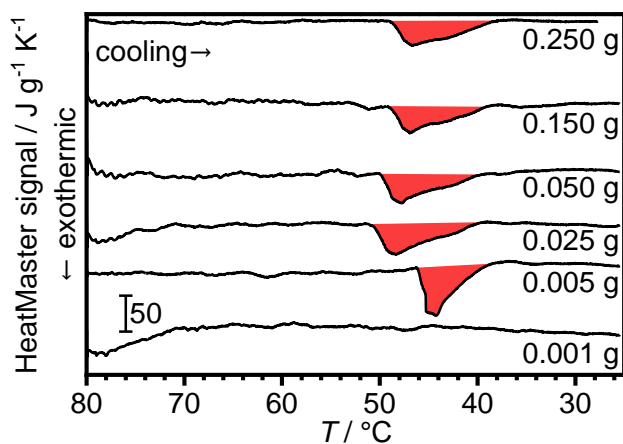
Figure 5. HeatMaster scans upon cooling 5 g sodium acetate trihydrate with different masses of $CaCl_2 \cdot 2H_2O$ as nucleating agent ranging from 0.250 to 0.001 g. The cooling rate was 0.5 °C min^{-1} and the crystallization exotherms are indicated by red-shaded areas.

In contrast to $CaCl_2 \cdot 2H_2O$, $MgCl_2 \cdot 6H_2O$ is a less reliable nucleating agent upon cycling SAT between 25 and 80 °C as shown in Figure 6 with heating scans in (a) and cooling scans in (b). Melting upon heating and crystallization upon cooling was observed only for the first two heating / cooling steps. After the third melting, the sample supercooled as can be seen from cooling scan (3). During the fourth heating scan, cold crystallization of the metastable supercooled liquid was observed at around 40 °C which was followed by melting above 50 °C. Upon cooling, all following cooling scans (4–10) show supercooling and cold crystallization followed by melting was seen for heating scans (5) and (8). This data shows that $MgCl_2 \cdot 6H_2O$ cannot act as a reliable nucleating agent for SAT after a few heating / cooling cycles with a maximum temperature of 80 °C.

11

Figure 6. HeatMaster scans of 5 g sodium acetate trihydrate with 0.25 g $MgCl_2 \cdot 6H_2O$ and 10 cycles. (a) Heating at 0.5 °C min^{-1} from 25 to 80 °C. (b) Cooling at 0.5 °C min^{-1} from 80 to 25 °C. Endotherms and exotherms are indicated by blue and red-shaded areas, respectively.

Using powder X-ray diffraction, it was confirmed that the crystallization products using both $CaCl_2 \cdot 2H_2O$ and $MgCl_2 \cdot 6H_2O$ are pure SAT as shown in Figure 7. This is an important test since SAA can be a byproduct of crystallization which degrades the performance of SAT as phase-change material. Figure 7 also shows that the SAT starting material used in our study is phase-pure SAT. When exotherms were absent after cooling, the samples were sometimes still found to contain some crystalline material at room temperature sometimes turning the supercooled SAT into a viscous gel. In line with previous observations,[14] this crystalline material is presumably SAA which crystallized without releasing detectable amounts of heat upon cooling. Attempts to characterize this material with XRD failed since opening of the glass vials typically resulted in the crystallization of SAT as noticed from the increase of temperature of the sample.
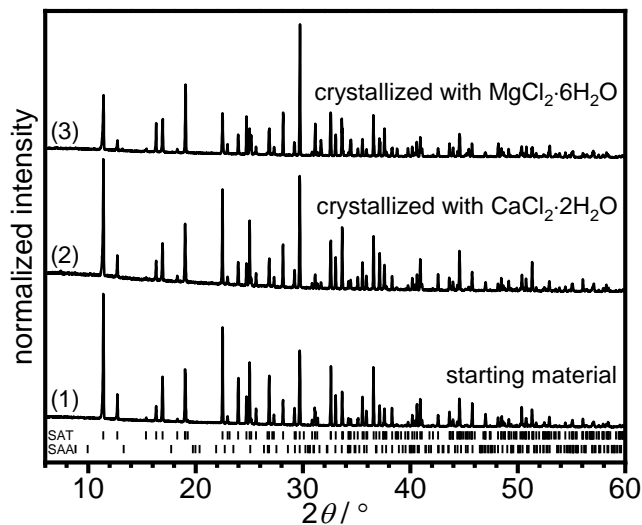
Figure 7. Power X-ray diffraction patterns (Cu Kα) of (1) the sodium acetate trihydrate starting material and sodium acetate trihydrate using (2) $CaCl_2 \cdot 2H_2O$ and (3) $MgCl_2 \cdot 6H_2O$ as nucleating agents. Tick marks indicate the expected positions of Bragg peaks of sodium acetate trihydrate[44, 45] and sodium acetate anhydrate.[46] Traces of the nucleating agents could not be detected in any of the samples.

Reinspection of the data shown in Figure 3 raises the question why crystallization of SAT was not observed using $Na_2HPO_4 \cdot 7H_2O$, $Na_2HPO_4 \cdot 12H_2O$ and $Na_4P_2O_7 \cdot 10H_2O$ which are well-known nucleating agents.[17, 18, 27, 34] Close inspection of the literature revealed that using 80 °C as the maximum temperature is quite harsh and that many of the known nucleating agents for SAT, including those based on sodium hydrogenphosphates, lose their performance at higher temperatures.[14, 27] This has been attributed to the loss of SAT crystals on the surfaces of the nucleating agents.[29] However, it also seems possible that the nucleating agents may undergo phase transitions to inactive materials or that they become fully soluble in the liquid SAT.

As a test, we reduced the maximum temperature to 65 °C for the heating / cooling cycles and used 0.25 g of $Na_2HPO_4 \cdot 12H_2O$ as the nucleating agent for 5 g SAT. As shown in Figure S6, and consistent with the literature, $Na_2HPO_4 \cdot 12H_2O$ was now indeed capable of inducing nucleation of SAT under these changed conditions. Equally, we found that the previously investigated $MgCl_2 \cdot 6H_2O$ (Figure 6) becomes a reliable nucleating agent when a maximum temperature of 65 °C is used as shown in Figure S7.

13

It can be concluded that $CaCl_2 \cdot 2H_2O$ is an excellent nucleating agent for SAT that performs well, unlike other nucleating agents, under quite harsh temperature conditions up to 80 °C. This could be a technological advantage since accidental heating of heat batteries containing other nucleating agents could effectively render them inactive. According to the binary phase diagram of $CaCl_2$ and H_2O,[47, 48] the dihydrate melts incongruently at 175 °C and is therefore perfectly stable under our conditions with maximum temperatures of 80 °C. The $CaCl_2$ hexahydrate on the other hand decomposes at 30.1 °C which is probably the reason why it does not act as a nucleating agent for SAT as shown in Figure 3.

Regarding the molecular details of the nucleation event at the $CaCl_2 \cdot 2H_2O$ / liquid SAT interface, it can be speculated that the carboxylate groups of acetate coordinate to calcium cations at the surface $CaCl_2 \cdot 2H_2O$ which then leads to nucleation and crystal growth of SAT. In this context, it is worth mentioning that calcium acetate monohydrate did not act as a nucleating agent for SAT as shown in Figure 3. A possible reason for this finding is that the local geometries of the acetate anions at the heterogenous interface are not capable of promoting crystal growth of SAT. Calcium carbonate (calcite) was also not able to crystallize SAT which could be due to either inaccessible calcium cations at the interface or unsuitable coordination geometries of acetate. Ultimately, the processes at the heterogenous interface can probably only be fully understood with the help of molecular dynamics simulations.

In a final step, the long-term performance of $CaCl_2 \cdot 2H_2O$ as a nucleating agent was benchmarked against $MgCl_2 \cdot 6H_2O$ and $Na_2HPO_4 \cdot 12H_2O$. These experiments were performed with maximum temperatures of 65 °C since the latter two nucleating agents would not work reliably otherwise. The experiments consisted of 50 heating / cooling cycles to test if the heat releases decrease upon thermal cycling. Such degradation effects limit the life time of heat batteries and need to be minimized as much as possible. For each of the nucleating agents, six samples were run in parallel which gives in total 300 cooling scans. The complete data from using $CaCl_2 \cdot 2H_2O$ as the nucleating agent is shown in Figure S8.

The onset temperatures, T_i, of the crystallization exotherms (see Figure 2(c) for definition) did not show systematic changes with respect to the number of cycles. The various datasets were therefore analyzed with the help of histograms as shown in Figure 8(a-c). $Na_2HPO_4 \cdot 12H_2O$ displays the highest onset temperatures with an average T_i of 52.4 °C. This is followed by $CaCl_2 \cdot 2H_2O$ and $MgCl_2 \cdot 6H_2O$ with average T_i values of 49.6 °C and 47.6 °C, respectively.

14

Interestingly, the $CaCl_2 \cdot 2H_2O$ data seems to be skewed towards higher temperatures with even a second maximum whereas the $MgCl_2 \cdot 6H_2O$ and $Na_2HPO_4 \cdot 12H_2O$ data are skewed towards lower temperatures. Given the large number of data points ($n = 300$), these effects are expected to be statistically significant yet they are not easily explained.
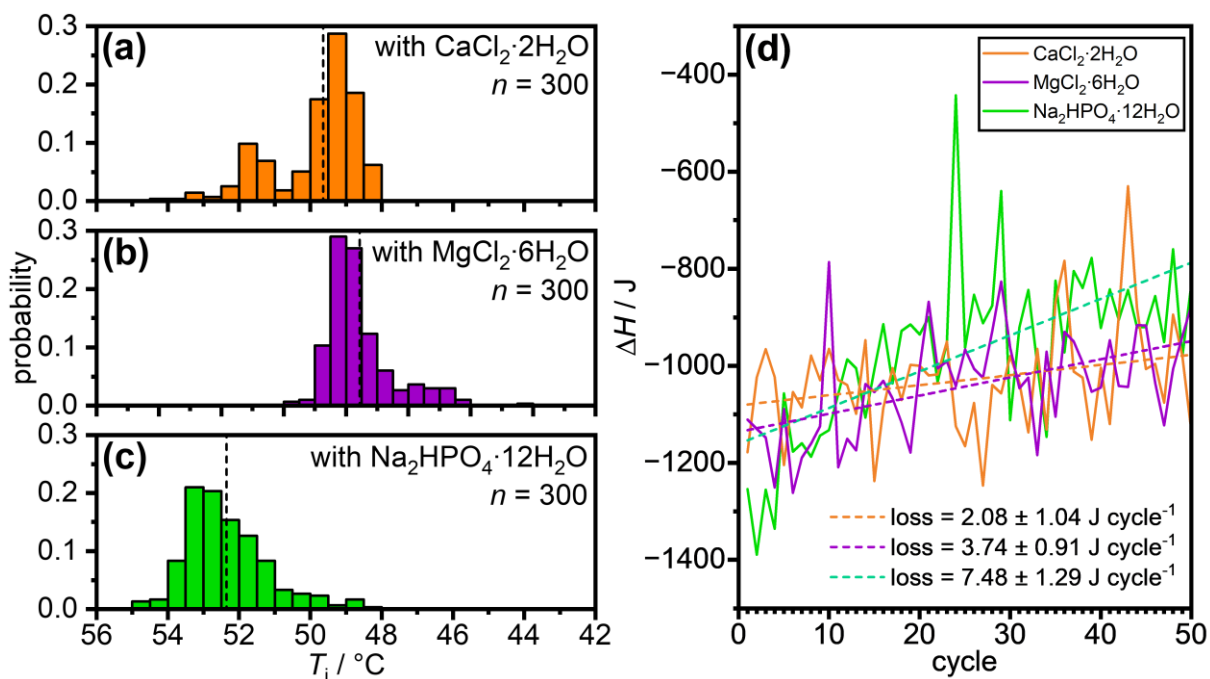
Figure 8. (a) Onset temperatures of crystallization of 5 g sodium acetate with 0.250 g of (a) $CaCl_2 \cdot 2H_2O$, (b) $MgCl_2 \cdot 6H_2O$ and (c) $Na_2HPO_4 \cdot 12H_2O$ as the nucleating agents upon cooling at 0.5 °C min^{-1} from 65 to 25 °C for 50 cycles and using 6 heating modules. The vertical dashed lines in (a-c) indicate the average temperatures. (d) Average heat releases from the 6 heating modules as the number of cycles increases to 50. Linear fits indicate the loss of performance for the phase-change material using the three different nucleating agents.

The areas of the various exotherms are shown as a function of the cycle number for the three nucleating agents in Figure 8(d). The data is somewhat noisy. However, error analysis of the slopes shows that they are all positive well outside of the margins of error indicating a degradation of the heat-release performance upon thermal cycling. The largest loss with 7.48 ± 1.29 J per cycle was observed using $Na_2HPO_4 \cdot 12H_2O$ as the nucleating agent. The best performance was found for the newly found $CaCl_2 \cdot 2H_2O$ nucleating agent with a loss of 2.08 ± 1.04 J per cycle.

Conclusions

15

$CaCl_2 \cdot 2H_2O$ is an excellent nucleating agent for SAT that remains active even after heating to 80 °C. Reliable performance is observed above 0.1 w%. $MgCl_2 \cdot 6H_2O$ on the other hand loses its ability to nucleate SAT after heating to 80 °C. However, upon using a maximum temperature of 65 °C a reliable performance was observed. In terms of degradation of the heat releases with increasing numbers of duty cycles, both $CaCl_2 \cdot 2H_2O$ and $MgCl_2 \cdot 6H_2O$ were found to display better characteristics compared to the commonly used $Na_2HPO_4 \cdot 12H_2O$ nucleating agent.

The extensive screening and performance-testing of nucleating agents for SAT was possible with the new HeatMaster instrument. Being able to measure samples on the gram scale bridges an important gap between the milligram-scale of differential scanning calorimetry and the kilogram-scale of commercial heat batteries. Its ability to measure several samples in parallel allows a high throughput of samples and obtaining good statistics with respect to onset temperatures and transition enthalpies. Furthermore, the HeatMaster could be easily integrated in a fully automated workflow including sample preparation, data analysis and data interpretation with the use of machine learning. Such an approach could lead to the discovery of new high-performance phase-change materials, nucleating agents and new strategies for improving their thermal conductivities.

ASSOCIATED CONTENT

Supporting Information

Additional experimental data showing the characteristics of the HeatMaster as well as additional nucleating experiments (PDF)

AUTHOR INFORMATION

Corresponding Author

* Department of Chemistry, University College London, London WC1H 0AJ, UK, Tel.: +44 7679 8864, Email: c.salzmann@ucl.ac.uk

ACKNOWLEDGEMENT

REFERENCES

(1) Sharma, S. D.; Sagara, K. Latent Heat Storage Materials and Systems: A Review. *Int. J. Green Energy* **2005**, *2*, 1-56.

(2) Kiyabu, S.; Girard, P.; Siegel, D. J. Discovery of Salt Hydrates for Thermal Energy Storage. *J. Am. Chem. Soc.* **2022**, *144*, 21617-21627.

(3) Odoi-Yorke, F.; Opoku, R.; Davis, F.; Obeng, G. Y. Optimisation of thermal energy storage systems incorporated with phase change materials for sustainable energy supply: A systematic review. *Energy Rep.* **2023**, *10*, 2496-2512.

(4) Liu, L.; Zhang, Y.; Zhang, S.; Tang, B. Advanced Phase Change Materials from Natural Perspectives: Structural Design and Functional Applications. *Adv. Sci.* **2023**, *10*, 2207652.

(5) Matuszek, K.; Kar, M.; Pringle, J. M.; MacFarlane, D. R. Phase Change Materials for Renewable Energy Storage at Intermediate Temperatures. *Chem. Rev.* **2023**, *123*, 491-514.

(6) Piper, S. L.; Forsyth, C. M.; Kar, M.; Gassner, C.; Vijayaraghavan, R.; Mahadevan, S.; Matuszek, K.; Pringle, J. M.; MacFarlane, D. R. Sustainable materials for renewable energy storage in the thermal battery. *RSC Sustain.* **2023**, *1*, 470-480.

(7) Chen, Y.; Xu, P.; Chen, Z.; Wang, H.; Sha, H.; Ji, Y.; Zhang, Y.; Dou, Q.; Wang, S. Experimental investigation of demand response potential of buildings: Combined passive thermal mass and active storage. *Appl. Energy* **2020**, *280*, 115956.

(8) Rozanna, D.; Chuah, T. G.; Salmiah, A.; Choong, T. S. Y.; Sa'ari, M. Fatty Acids as Phase Change Materials (PCMs) for Thermal Energy Storage: A Review. *Int. J. Green Energy* **2005**, *1*, 495-513.

(9) Purohit, B. K.; Sistla, V. S. Inorganic salt hydrate for thermal energy storage application: A review. *Energy Storage* **2021**, *3*, e212.

(10) Khadiran, T.; Hussein, M. Z.; Zainal, Z.; Rusli, R. Advanced energy storage materials for building applications and their thermal performance characterization: A review. *Renew. Sustain. Energy Rev.* **2016**, *57*, 916-928.

(11) Kenisarin, M.; Mahkamov, K. Salt hydrates as latent heat storage materials: Thermophysical properties and costs. *Sol. Energy Mater. Sol. Cells* **2016**, *145*, 255-286.

(12) Alva, G.; Liu, L.; Huang, X.; Fang, G. Thermal energy storage materials and systems for solar energy applications. *Renew. Sustain. Energy Rev.* **2017**, *68*, 693-706.

17

(13) Wang, Z.; Liu, S.; Ma, G.; Xie, S.; Du, G.; Sun, J.; Jia, Y. Preparation and properties of caprylic-nonanoic acid mixture/expanded graphite composite as phase change material for thermal energy storage. *Int. J. Energy Res.* **2017**, *41*, 2555-2564.

(14) Naumann, R.; Emons, H. H. Results of thermal analysis for investigation of salt hydrates as latent heat-storage materials. *J. Thermal Anal.* **1989**, *35*, 1009-1031.

(15) Sharma, A.; Tyagi, V. V.; Chen, C. R.; Buddhi, D. Review on thermal energy storage with phase change materials and applications. *Renew. Sustain. Energy Rev.* **2009**, *13*, 318-345.

(16) Beaupere, N.; Soupremanien, U.; Zalewski, L. Nucleation triggering methods in supercooled phase change materials (PCM), a review. *Thermochim. Acta* **2018**, *670*, 184-201.

(17) Cabeza, L. F.; Svensson, G.; Hiebler, S.; Mehling, H. Thermal performance of sodium acetate trihydrate thickened with different materials as phase change energy storage material. *Appl. Therm. Eng.* **2003**, *23*, 1697-1704.

(18) Mao, J.; Dong, X.; Hou, P.; Lian, H. Preparation research of novel composite phase change materials based on sodium acetate trihydrate. *Appl. Therm. Eng.* **2017**, *118*, 817-825.

(19) Kong, W.; Dannemand, M.; Johansen, J. B.; Fan, J.; Dragsted, J.; Englmair, G.; Furbo, S. Experimental investigations on heat content of supercooled sodium acetate trihydrate by a simple heat loss method. *Sol. Energy* **2016**, *139*, 249-257.

(20) Xiao, Q.; Fan, J.; Li, L.; Xu, T.; Yuan, W. Solar thermal energy storage based on sodium acetate trihydrate phase change hydrogels with excellent light-to-thermal conversion performance. *Energy* **2018**, *165*, 1240-1247.

(21) Su, W.; Darkwa, J.; Kokogiannakis, G. Review of solid–liquid phase change materials and their encapsulation technologies. *Renew. Sustain. Energy Rev.* **2015**, *48*, 373-391.

(22) Huang, J.; Wang, T.; Zhu, P.; Xiao, J. Preparation, characterization, and thermal properties of the microencapsulation of a hydrated salt as phase change energy storage materials. *Thermochim. Acta* **2013**, *557*, 1-6.

(23) Dannemand, M.; Johansen, J. B.; Furbo, S. Solidification behavior and thermal conductivity of bulk sodium acetate trihydrate composites with thickening agents and graphite. *Sol. Energy Mater. Sol. Cells* **2016**, *145*, 287-295.

(24) Lizana, J. C., R.; Barrios-Padura, A.; Valverde, J.M.; Ortiz, C. Identification of best available thermal energy storage compounds for low-to-moderate temperature storage applications in buildings. *Mater. Construcc.* **2018**, *68*, e160.

18

(25) Lizana, J.; Sanchez-Jimenez, P. E.; Chacartegui, R.; Becerra, J. A.; Perez-Maqueda, L. A. Supercooled sodium acetate aqueous solution for long-term heat storage to support heating decarbonisation. *J. Energy Storage* **2022**, *55*, 105584.

(26) Pebler, A. Dissociation vapor pressure of sodium acetate trihydrate. *Thermochim. Acta* **1975**, *13*, 109-114.

(27) Oliver, D. E.; Bissell, A. J.; Liu, X.; Tang, C. C.; Pulham, C. R. Crystallisation studies of sodium acetate trihydrate - suppression of incongruent melting and sub-cooling to produce a reliable, high-performance phase-change material. *CrystEngComm* **2021**, *23*, 7-76.

(28) Guion, J.; Teisseire, M. Nucleation of sodium acetate trihydrate in thermal heat storage cycles. *Solar energy* **1991**, *46*, 97-100.

(29) Wada, T.; Matsuo, Y. Studies on Salt Hydrates for Latent Heat Storge. VI. Preheating Effect on Crystallization of Sodium Acetate Trihydrate from Aqueous Solution with a Small Amount of Disodium Hydrogenphosphate. *Bull. Chem. Soc. Jpn.* **1984**, *57*, 561-563.

(30) Kumar, N.; Hirschey, J.; LaClair, T. J.; Gluesenkamp, K. R.; Graham, S. Review of stability and thermal conductivity enhancements for salt hydrates. *J. Energy Storage* **2019**, *24*, 100794.

(31) Wada, T.; Yamamoto, R.; Matsuo, Y. Heat storage capacity of sodium acetate trihydrate during thermal cycling. *Sol. Energy* **1984**, *33*, 373-375.

(32) Green, W. F. The "Melting-Point" of Hydrated Sodium Acetate: Solubility Curves. *J. Phys. Chem.* **1908**, *12*, 655-660.

(33) Wada, T.; Yamamoto, R. Studies on Salt Hydrate for Latent Heat Storage. I. Crystal Nucleation of Sodium Acetate Trihydrate Catalyzed by Tetrasodium Pyrophosphate Decahydrate. *Bull. Chem. Soc. Jpn.* **1982**, *55*, 3603-3606.

(34) Mao, J.; Hou, P.; Liu, R.; Chen, F.; Dong, X. Preparation and thermal properties of SAT-CMC-DSP/EG composite as phase change material. *Appl. Therm. Eng.* **2017**, *119*, 585-592.

(35) Ryu, H. W.; Woo, S. W.; Shin, B. C.; Kim, S. D. Prevention of supercooling and stabilization of inorganic salt hydrates as latent heat storage materials. *Sol. Energy Mater. Sol. Cells* **1992**, *27*, 161-172.

(36) Li, X.; Zhou, Y.; Nian, H.; Zhu, F.; Ren, X.; Dong, O.; Hai, C.; Shen, Y.; Zeng, J. Preparation and thermal energy storage studies of CH3COONa·3H$_2$O–KCl composites salt system with enhanced phase change performance. *Appl. Therm. Eng.* **2016**, *102*, 708-715.

19

(37) Cui, W.; Yuan, Y.; Sun, L.; Cao, X.; Yang, X. Experimental studies on the supercooling and melting/freezing characteristics of nano-copper/sodium acetate trihydrate composite phase change materials. *Renew. Energy* **2016**, *99*, 1029-1037.

(38) Garay Ramirez, B. M. L.; Glorieux, C.; San Martin Martinez, E.; Flores Cuautle, J. J. A. Tuning of thermal properties of sodium acetate trihydrate by blending with polymer and silver nanoparticles. *Appl. Therm. Eng.* **2014**, *62*, 838-844.

(39) Hu, P.; Lu, D.-J.; Fan, X.-Y.; Zhou, X.; Chen, Z.-S. Phase change performance of sodium acetate trihydrate with AlN nanoparticles and CMC. *Sol. Energy Mater. Sol. Cells* **2011**, *95*, 2645-2649.

(40) Liu, C.; Hu, P.; Xu, Z.; Ma, X.; Rao, Z. Experimental investigation on thermal properties of sodium acetate trihydrate based phase change materials for thermal energy storage. *Thermochim. Acta* **2019**, *674*, 28-35.

(41) Stunić, Z.; Djuriĉković, V.; Stunić, Z. Thermal storage: Nucleation of melts of inorganic salt hydrates. *J. Appl. Chem. Biotechnol.* **1978**, *28*, 761-764.

(42) Fashandi, M.; Leung, S. N. Sodium acetate trihydrate-chitin nanowhisker nanocomposites with enhanced phase change performance for thermal energy storage. *Sol. Energy Mater. Sol. Cells* **2018**, *178*, 259-265.

(43) Dannemand, M.; Dragsted, J.; Fan, J.; Johansen, J. B.; Kong, W.; Furbo, S. Experimental investigations on prototype heat storage units utilizing stable supercooling of sodium acetate trihydrate mixtures. *Appl. Energy* **2016**, *169*, 72-80.

(44) Cameron, T. S.; Mannan, K. M.; Rahman, M. O. The crystal structure of sodium acetate trihydrate. *Acta Cryst.* **1976**, *B32*, 87-90.

(45) Wei, K.-T.; Ward, D. L. Sodium acetate trihydrate: a redetermination. *Acta Cryst.* **1977**, *B33*, 522-526.

(46) Hsu, L.-Y.; Nordman, C. E. Structures of two forms of sodium acetate, $Na^+.C2H3O2^-$. *Acta Cryst.* **1983**, *C39*, 690-694.

(47) Baumgartner, M.; Bakker, R. J. $CaCl_2$-hydrate nucleation in synthetic fluid inclusions. *Chem. Geol.* **2009**, *265*, 335-344.

(48) Brady, J. B. Magma in a beaker: Analog Experiments with water and various salts or sugar for teaching igneous petrology. *Canad. Mineral.* **2009**, *47*, 457-471.

For Table of Contents Use